Pacific Northwest
NATIONAL LABORATORY

PNNL-38379

Vibrational signatures of S vacancies in monolayer tungsten disulfide

September 2025

Micah P Prange

U.S. DEPARTMENT of ENERGY

Prepared for the U.S. Department of Energy
under Contract DE-AC05-76RL01830

DISCLAIMER

PACIFIC NORTHWEST NATIONAL LABORATORY
operated by
BATTELLE
for the
UNITED STATES DEPARTMENT OF ENERGY
under Contract DE-AC05-76RL01830

Printed in the United States of America

Available to DOE and DOE contractors from
the Office of Scientific and Technical Information,
P.O. Box 62, Oak Ridge, TN 37831-0062
www.osti.gov
ph: (865) 576-8401
fox: (865) 576-5728
email: reports@osti.gov

Available to the public from the National Technical Information Service
5301 Shawnee Rd., Alexandria, VA 22312
ph: (800) 553-NTIS (6847)
or (703) 605-6000
email: info@ntis.gov
Online ordering: http://www.ntis.gov

PNNL-38379

Vibrational signatures of S vacancies in monolayer tungsten disulfide

September 2025

Micah P Prange

Prepared for
the U.S. Department of Energy
under Contract DE-AC05-76RL01830

Pacific Northwest National Laboratory
Richland, Washington 99354

Abstract

S vacancies in WS_2 affect material performance but a difficult to detect. In this work we use theoretical simulations to predict the vibrational frequencies associated with S vacancies in monolayer WS_2. We report the phonon spectrum and band structure of the isolated monolayer and the frequencies that are introduced to the spectrum when a vacancy is created.

1.0 Summary

DFT phonon calculations show that V_S affect the vibrational structure of monolayer WS_2. A W breathing mode near 148 cm^{-1} is a likely candidate to mediate electron trapping.

Acknowledgments

This research was supported by the AT SCALE Initiative, under the Laboratory Directed Research and Development (LDRD) Program at Pacific Northwest National Laboratory (PNNL). PNNL is a multi-program national laboratory operated for the U.S. Department of Energy (DOE) by Battelle Memorial Institute under Contract No. DE-AC05-76RL01830.

Acronyms and Abbreviations

BZ	Brillouin zone
DFT	density functional theory
DOS	density of states
TMD	transition metal dichalcogenide

Contents

Abstract ii
Summary iii
Acknowledgments iv
Acronyms and Abbreviations v
1.0 Introduction 1
2.0 Methods 2
3.0 Results and discussion 3
3.1 Pristine monolayer WS_2 3
3.2 Monolayer WS_{2-x} with S vacancies 4
4.0 Conclusions 6
5.0 References 7

Figures

Figure 1. Phonon DOS (black) and zone-center vibrational frequencies (blue) of monolayer WS_2 calculated within DFPT. The irreducible representation with which each of the zone-center phonons transform is labelled, and the Raman activity is indicated by short (inactive) or long (active) vertical lines. 3

1.0 Introduction

Achieving a realistic materials-by-design implementation capable of producing customizable, high-quality materials at device scale requires control over nucleation and growth reactions to control stoichiometry, defect populations, crystal size, crystal symmetry, etc. The difficulty of this control represents a challenge to exploring large composition and structural spaces in emerging materials classes for novel technologies. Transition metal dichalcogenides (TMDs) are one such class: many exotic phenomena have been observed or predicted but developing a robust understanding of the structure-function relationships has been hampered by the slow pace of device construction, which has been done to-date by brute force trial-and-error. This approach is inefficient for discovering new functional materials in the large space of material parameters, especially when defects, structural distortions, and other inhomogeneities strongly affect properties of interest as in TMDs. Automated and autonomous synthetic routes using chemical vapor deposition and transport of layered TMDs may be a promising route to control defect speciation and density during crystal growth. This possibility, however, is contingent on some feedback information channel by which the synthesis can be guided as it progresses. Vibrational and vibronic spectroscopies represent one conceivable such information conduit, but it has yet to be demonstrated either experimentally or theoretically. In this report, I present theoretical calculations of the phonon spectrum of pristine and sulfur deficient monolayer WS_2 crystals using density functional theory (DFT) as implemented in two popular electronic structure packages. The phonon dispersion is calculated along high symmetry lines for the pristine case, phonon densities of states (DOS) are calculated for pristine and defective models, and the effects of the vacancy defect are discussed. This work suggests that local vibrational modes around sulfur vacancies have diagnostic local vibrations in the ultralow frequency (~150 cm^{-1}).

2.0 Methods

Calculations were performed with the Vienna ab initio simulation package (VASP (Kresse and Furthmuller 1996b, 1996a)) using the projector-augmented wave (PAW) (Blöchl 1994; Kresse and Joubert 1999) approach to soften the Kohn-Sham potentials. The PBE exchange-correlation functional was used (Perdew, Burke, and Ernzerhof 1996). The energy cutoff was set to 323.4 eV. Monolayer models were constructed by cleaving a single layer from the relaxed bulk. The cell was 13.5 Å in the direction normal to the monolayer. To model the S vacancy, a 3x3x1 supercell was constructed and a single S atom was removed. All of the S atoms in the nondefective monolayer are equivalent. 11x11x2 and 2x2x2 k-point grids were used with the small and large cells, respectively. The finite difference method was used to generate the force constants, and the phonopy package(Togo 2022) (Togo et al. 2023) was used to calculate the dynamical matrix and phonon properties.

3.0 Results and discussion

3.1 Pristine monolayer WS_2

Monolayer WS_2 has one formula unit per unit cell and belongs to space group P3m1. Hence it has 9 phonon modes at a general wavevector. The density of states (DOS) of the computed phonon spectrum (Figure 1) and the phonon dispersion relation along the path $\Gamma \rightarrow K \rightarrow M$ (Figure 2) where Γ=(0,0,0), K=(1/3,1/3,0), and M=(1/2, 0, 0) are high symmetry points expressed in fractional coordinates in the first Brillouin zone (BZ) are shown. There is a gap between the three acoustic modes and the 6 optical modes. At Γ the lowest two optical modes are both double degenerate, giving 4 distinct long-wavelength vibrational frequencies. The middle two of these are Raman active. Our simulations predict the active modes to to be at 345 and 407 cm^{-1}. These compare well observed Raman peaks at 352.5 and 414.9 cm^{-1} (Norden et al. 2019). This comparison establishes that the methods used here accurately capture the vibrational physics in WS_2 monolayers. The two prominent peaks in the acoustic bands around 140 and 175 cm^{-1} can be associated with the BZ boundary.

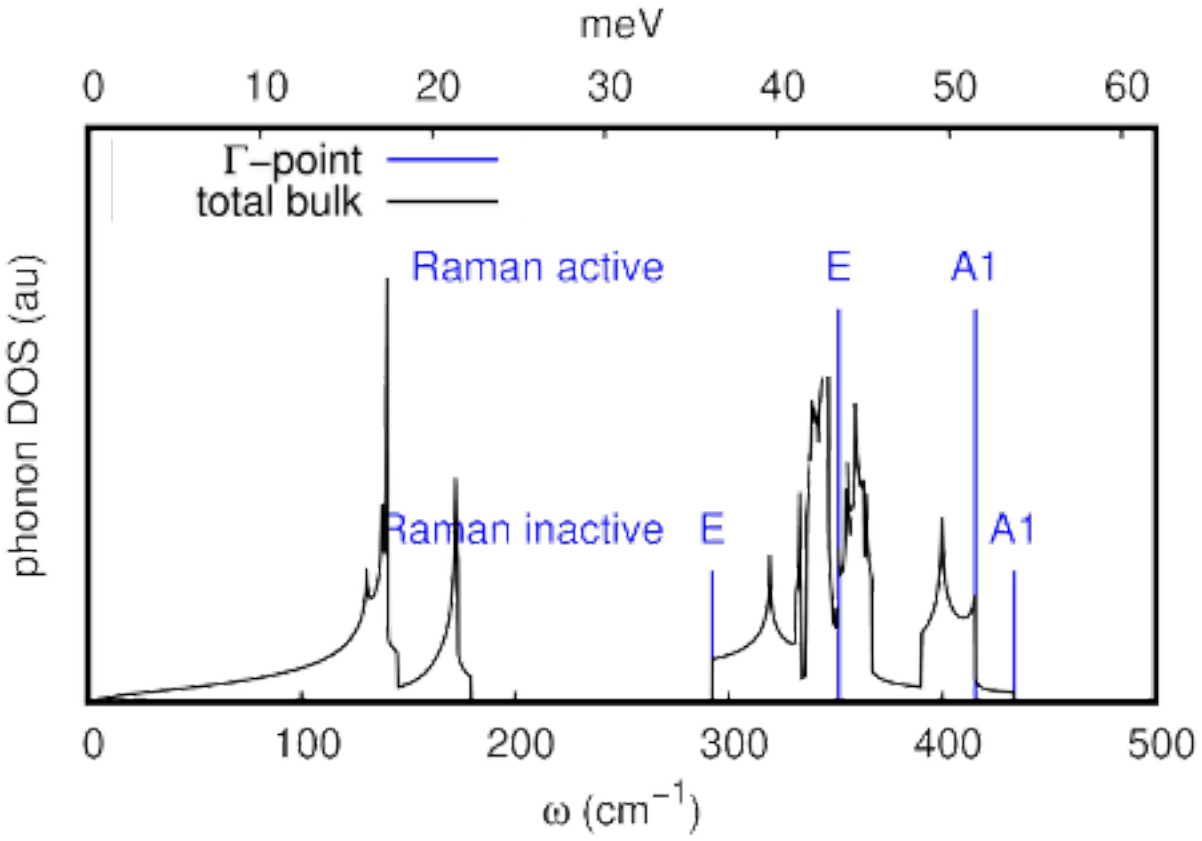

Figure 1. Phonon DOS (black) and zone-center vibrational frequencies (blue) of monolayer WS_2 calculated within DFPT. The irreducible representation with which each of the zone-center phonons transform is labelled, and the Raman activity is indicated by short (inactive) or long (active) vertical lines.

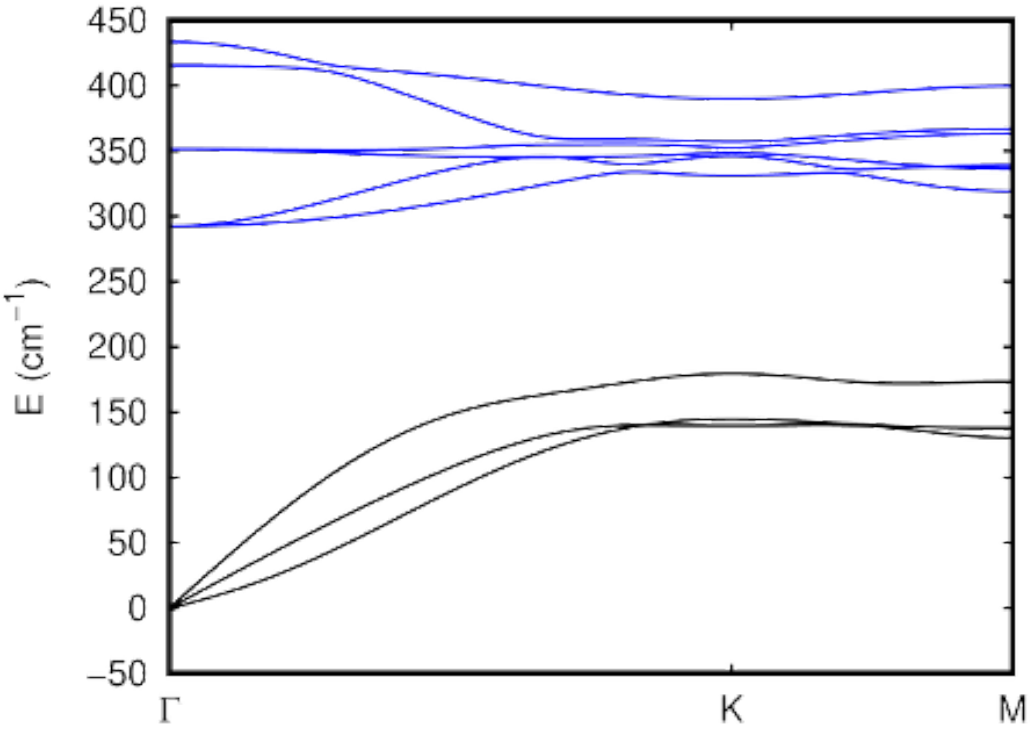

Figure 2. Phonon band structure of monolayer WS_2 showing acoustic modes in black and optical modes in blue.

3.2 Monolayer WS_{2-x} with S vacancies

The internal coordinates of the 3X3 lateral supercell with one of the 18 S atoms removed was relaxed, and the phonons were computed using the same procedure as used for the primitive pristine cell. The resulting DOS is shown in Figure 3. Most features of the vibrational structure of the nondefective monolayer are reproduced in the spectrum of the defective supercell. The acoustic and optical bands are clearly separated and occur at around the Additional bands, localized around the vacancy site, are also observed. We draw attention to the regions just below the lower edge of the optical band (approximately 280-295 cm^{-1}) and between the two prominent peaks in the acoustic bands (approximately 140-170 cm^{-1}). These regions host vibrations dominated by motion of the S atoms and W atoms, respectively. The lowest energy peaks (at 148 and 287 cm^{-1}) are marked in Figure 3. The eigenvectors of the dynamical matrix corresponding to these modes were inspected. The lower energy mode was determined to be a symmetric breathing mode of in-plane motions of W sublattice in which the 3 W atoms coordinating the vacancy move radially toward and away from the V_S site in synchronicity, suggesting that this mode may support the trapping of negative charges (electrons) on the vacancy site.

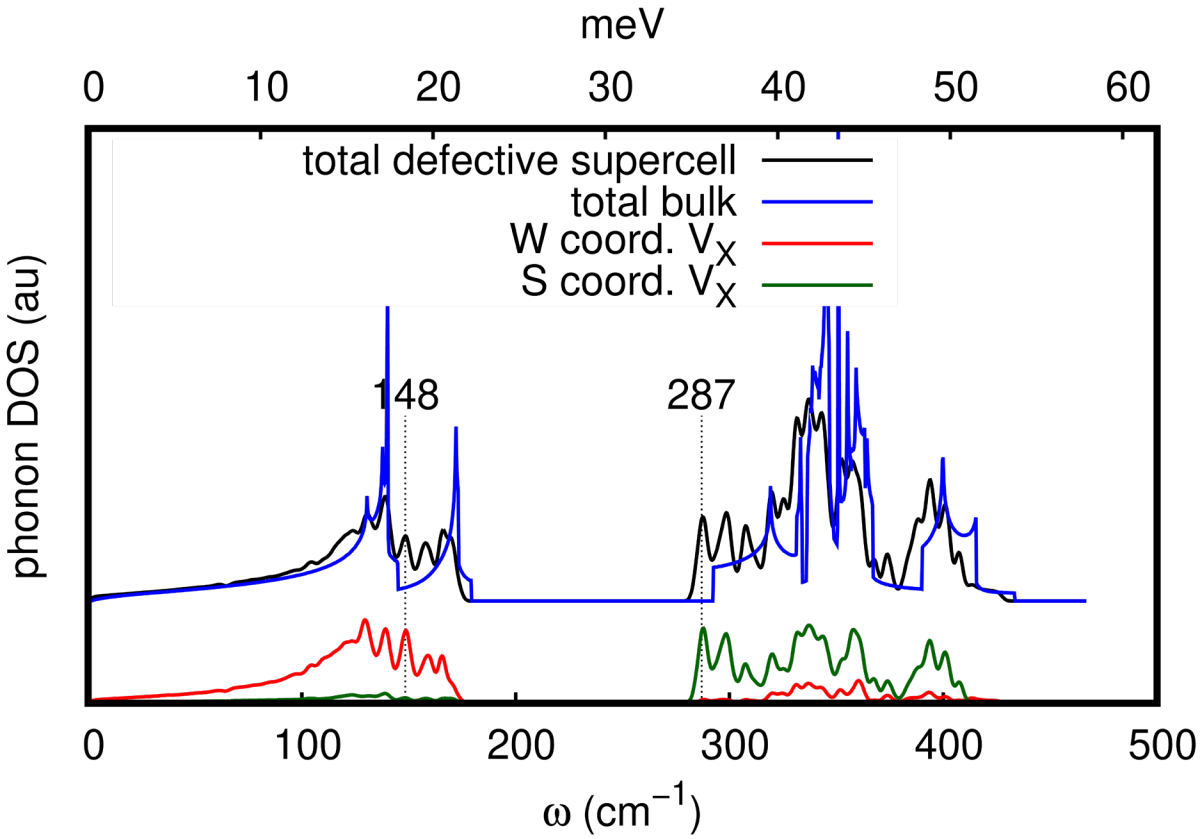

Figure 3. Phonon DOS with (black) and without (blue) S vacancies, and the DOS with vacancies projected onto W (red) and S (green) atoms coordinating the vacancy site. Localized modes belonging to the vacancy are labelled at 148 and 287 cm^{-1}.

4.0 Conclusions

We have performed DFT frozen phonon calculations of pristine and S deficient WS_2 monolayers. The resulting phonon classifications suggest that V_S in WS2 hosts localized vibrational modes near 148 and 287 cm^{-1} and that the lower energy mode can trap electrons. These vibrations may be a useful, spectroscopically detectable probe of local structure.

5.0 References

Blöchl, P.E. 1994. "Projector augmented-wave method." *Physical Review B* 50: 17953-17979. https://doi.org/http://dx.doi.org/10.1103/PhysRevB.50.17953.

Kresse, G., and J. Furthmuller. 1996a. "Efficiency of ab-initio total energy calculations for metals and semiconductors using a plane-wave basis set." *Computational Materials Science* 6: 15-50. https://doi.org/http://dx.doi.org/10.1016/0927-0256(96)00008-0.

---. 1996b. "Efficient iterative schemes for ab initio total-energy calculations using a plane-wave basis set." *Physical Review B* 54: 11169-11186. https://doi.org/http://dx.doi.org/10.1103/PhysRevB.54.11169.

Kresse, G., and D. Joubert. 1999. "From ultrasoft pseudopotentials to the projector augmented-wave method." *Physical Review B* 59: 1758-1775. https://doi.org/http://dx.doi.org/10.1103/PhysRevB.59.1758.

Norden, Tenzin, Chuan Zhao, Peiyao Zhang, Renat Sabirianov, Athos Petrou, and Hao Zeng. 2019. "Giant valley splitting in monolayer WS2 by magnetic proximity effect." *Nature Communications* 10 (1): 4163. https://doi.org/10.1038/s41467-019-11966-4. https://doi.org/10.1038/s41467-019-11966-4.

Perdew, J.P., K. Burke, and M. Ernzerhof. 1996. "Generalized gradient approximation made simple." *Physical Review Letters* 77 (18): 3865-3868. https://doi.org/http://dx.doi.org/10.1103/PhysRevLett.77.3865.

Togo, Atsushi. 2022. "First-principles Phonon Calculations with Phonopy and Phono3py." *Journal of the Physical Society of Japan* 92 (1): 012001. https://doi.org/10.7566/JPSJ.92.012001. https://doi.org/10.7566/JPSJ.92.012001.

Togo, Atsushi, Laurent Chaput, Terumasa Tadano, and Isao Tanaka. 2023. "Implementation strategies in phonopy and phono3py." *Journal of Physics: Condensed Matter* 35 (35): 353001. https://doi.org/10.1088/1361-648X/acd831. https://dx.doi.org/10.1088/1361-648X/acd831.

Pacific Northwest National Laboratory

902 Battelle Boulevard
P.O. Box 999
Richland, WA 99354

1-888-375-PNNL (7665)

www.pnnl.gov